

Structural and phonon properties of bundled single- and double-wall carbon nanotubes under pressure

A. L. Aguiar^{1,2}, Rodrigo B. Capaz³, A. G. Souza Filho,¹

A. San-Miguel²

¹*Departamento de Física, Universidade Federal do Ceará,*

P.O. Box 6030, 60455-900 Fortaleza, Ceará, Brazil

²*Laboratoire de Physique de la Matière Condensée et Nanostructures,*

Université Claude Bernard Lyon-1 et CNRS,

69622 Villeurbanne Cedex, France and

³*Instituto de Física, Universidade Federal do Rio de Janeiro,*

P.O.Box 68528, 22941-972, Rio de Janeiro, RJ, Brazil

(Dated: November 5, 2018)

Abstract

In this work, we report a theoretical coupled study of the structural and phonons properties of bundled single- and double-walled carbon nanotubes (DWNTs), under hydrostatic compression. Our results confirm drastic changes in volume of SWNTs in high-pressure regime as assigned by a phase transition from circular to collapsed phase which are strictly dependent on the tube diameter. For the DWNTs, those results show first a transformation to a polygonized shape of the outer tube and subsequently the simultaneous collapse of the outter and inner tube, at the onset of the inner tube ovalization. Before the DWNT collapse, phonon calculations reproduce the experimentally observed screening effect on the inner tube pressure induced blue shift both for RBM and tangential G_z modes . Furthermore, the collapse of CNTs bundles induces a sudden redshift of tangential component in agreement with experimental studies. The G_z band analysis of the SWNT collapsed tubes shows that the flattened regions of the tubes are at the origin of their G-band signal. This explains the observed graphite type pressure evolution of the G band in the collapsed phase and provides in addition a mean for the identification of collapsed tubes.

I. INTRODUCTION

Carbon nanotubes are fundamental materials for developing nanoelectromechanical systems because they present a unique combination of outstanding electronic and mechanical properties. Cross-sectional deformations of single-wall carbon nanotubes (SWNTs) under pressure have been extensively studied by means of experimental tools¹⁻⁵ and theoretical models.⁶⁻¹² On the other hand, the behavior of double-wall carbon nanotubes (DWNTs) under pressure has been considerably less studied¹³⁻¹⁶. DWNTs may be better candidate materials than SWNTs for the engineering of nanotube-based composite materials because of their geometry, in which the outer tube ensures the chemical coupling with the matrix and the inner tube acts as mechanical support for the whole system¹⁷.

Some theoretical studies have been performed to study the pressure dependence of the cross-sectional shape of SWNT, depending on the chirality and diameter. By starting from an almost perfect circular cross section, the cross-sectional shape of the nanotube becomes oval or polygonized as the pressure is increased, evolving later to a collapsed state with a peanut shape.^{11,18-21} Based on elasticity theory, Sluiter et al. have proposed a diameter-dependent phase diagram for the cross-sectional shape of SWNTs under pressure.²² Some authors reported that the radial deformation of SWNTs for diameters smaller than 2.5nm is reversible from the collapsed state while the deformation of larger diameter tubes could be irreversible and the collapsed state is metastable or even absolutely stable without pressure application.^{11,22} Many experimental studies have suggested that phase transition in nanotubes could be dependent on their metallic character or on the surrounding chemical environment used for transmitting the pressure.^{4,23-26} However, theoretical calculations suggest that phase transitions of SWNTs under pressure is mainly dependent on the cube inverted diameter ($p_c \sim d_t^{-3}$) of the tubes and not on the chirality.^{11,27} Even if there is a huge dispersion of results concerning the pressure transition values from theoretical models, there is an overall agreement between different calculations on the existence of two phase transitions (circular-oval and oval-peanut) and that the critical pressures for those transitions are diameter dependent.

The pressure evolution of DWNTs has been much less studied and, in opposition to SWNTs, a detailed understanding of their cross-sectional evolution is still under discussion due their complexity regarding the role of inner and outer tubes. Ye et al. has suggested that

the critical collapse pressure of DWNT is essentially determined by inner tube stability and so the collapse pressure of DWNT is close to what is expected for inner tube²⁸. Other authors suggested that collapse pressure of DWNTs is completely different from which is expected for the correspondent SWNT when are considerate separately and, the pressure value still depends on $1/d_t^{*3}$ scale law but with a suitable choice of an average diameter $d_t^{*29,30}$. In this paper we report a study of the vibrational properties of carbon nanotubes bundle under pressure, a subject that has not been theoretically well explored in the literature up to now.

This paper is organized as follows. First, we will describe in section II the methodology used to model nanotube bundled structure. In section III.A, we calculated the structural evolution of SWNTs and DWNTs bundles under pressure. We focused in structural stability of bundle structure by calculating the critical pressure for collapsing and we compare the behavior of DWNT bundle with its corresponding SWNT. In section III.B, we explored the vibrational properties of SWNT and DWNTs bundle under pressure by calculating RBM and tangential phonons modes before and after the nanotube collapse. We close our paper with conclusions in section IV.

II. METHODOLOGY

In order to access mechanical and vibrational properties of carbon nanotubes under pressure we initially perform zero-temperature structural minimizations of SWNTs and DWNTs bundles. The carbon-carbon bonding within each CNTs is modeled by a reactive empirical bond order (REBO) potential proposed by Brenner^{31,32}. Pairwise Lennard-Jones potentials are added to model the non-bonding van der Waals terms ($\epsilon/k_b=44\text{K}$, $\sigma = 3.39 \text{ \AA}$), which are essential to describe intertube interactions¹¹. We studied zigzag and armchair C bundles of CNTs in triangular arrangements within orthogonal unit cells containing two SWNTs or DWNTs each, with lateral lattice constants a_x and $a_y = \sqrt{3}a_x$ (the a_y/a_x ratio is kept fixed). The lattice constant along the z axis, (a_z), is chosen to contain 5 (8) unit cells of the zigzag (armchair) tubes.

We perform a sequence of small and controllable steps of unit cell volume reduction for each fixed nanotube phase studied (circular, polygonized, oval, peanut,etc.). Each step is of the order of $\Delta V/V_0 = -0.01\%$, where V_0 is the ambient pressure volume for each nanotube system in circular phase. For each fixed volume V , we search for the atomic positions and

lattice constants a_x and a_z that minimize the internal energy $U(V)$. The pressure is obtained by $p = -\Delta U/\Delta V$ and the enthalpy is $H = U + pV$.

Phonon frequencies and eigenvectors are directly obtained by the diagonalization of the force constant matrix. The matrix elements are calculated by using finite difference techniques. We focus our vibrational analysis on the radial breathing mode (RBM) and longitudinal G-band (denoted G_z), whose displacements are along the tube axis. Therefore, RBM and G_z projected density of states (PDOS) are constructed by projecting the phonon eigenvectors onto the corresponding radial and axial (with opposite phases for atoms in different sub-lattices) displacement fields, respectively.

III. SWNTS AND DWNTS UNDER PRESSURE: STRUCTURAL AND VIBRATIONAL PROPERTIES

A. Nanotube Collapse

We start by studying the low-pressure behavior of SWNT bundles, considering four basic cross-sectional shapes namely: circular, oval, polygonal (hexagonal) and peanut-like. Tubes of different diameters exhibit a different sequence of cross-sectional shapes as a function of pressure¹¹. In particular, the polygonal or hexagonal phase is typical of bundled tubes and it is often obtained in calculations for large diameter nanotubes since plane-parallel facing between adjacent tubes tends to decrease the van der Waals interaction energy³³⁻³⁵. Fig 1a shows the enthalpy as a function of pressure calculated for circular, oval and polygonized phases for bundles of (8,8), (18,0) and (24,0) SWNTs. The crossing of two curves in this plot by following the lowest enthalpy for a given pressure indicates a transition between two different cross-sectional shapes. The derivative discontinuities in the $H(p)$ plots are associated with the volume variation at the phase transition. This can be seen more clearly when $p - V$ plots are constructed (not shown here) where each transition is marked by a discontinuous change in volume. For the (8,8) SWNT bundle, the transition pressure from circular to oval (so called p_1) occurs close to 1.5 GPa and from oval to peanut (so called p_2) around 2.6 GPa. For the (18,0) SWNT bundle, we found phase transitions at 1.2 GPa (circular to polygonal, p'_1) and 1.5 GPa (polygonal to peanut, p'_2). Finally, for the (24,0) SWNT bundle the polygonal to peanut transition (p'_2) is found at 0.6 GPa. We see that

the small diameter (8,8) SWNT bundle undergoes a circular \rightarrow oval \rightarrow peanut phase transition sequence as the pressure increases, whereas for the intermediate diameter (18,0) SWNT the sequence is circular \rightarrow polygonal \rightarrow peanut and for the large-diameter (24,0) we obtain simply a polygonal-peanut transition, since the tubes are already polygonized even at zero pressure.

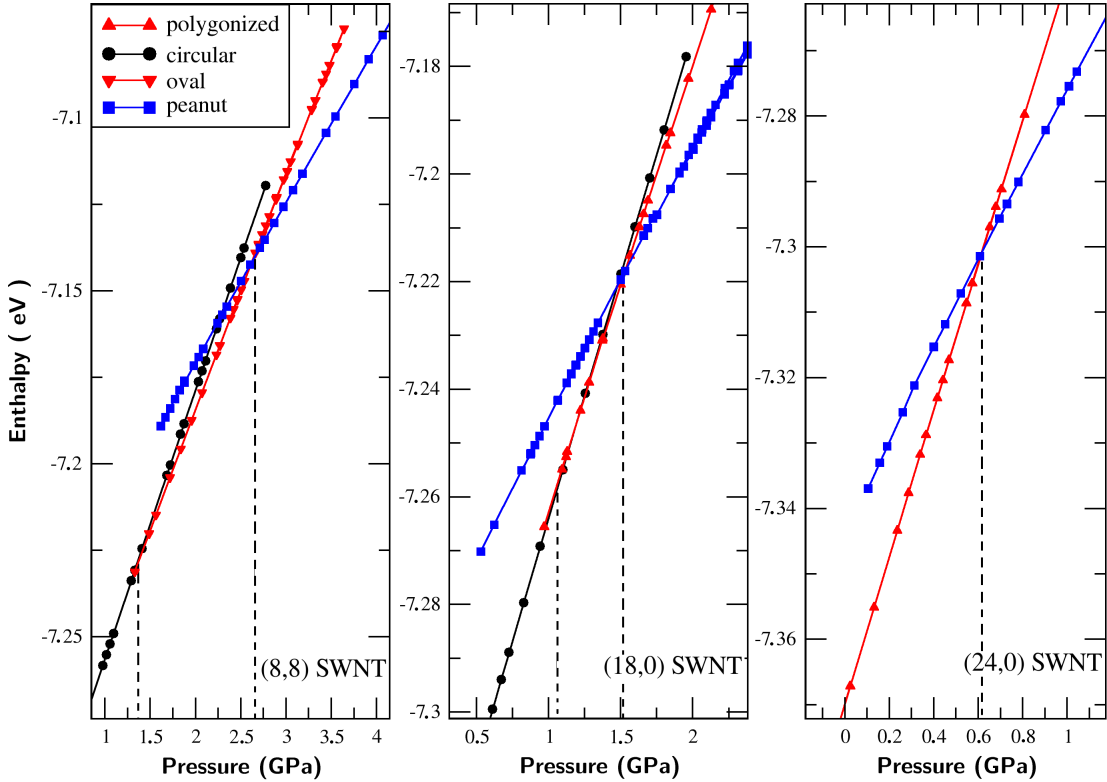


FIG. 1. Enthalpy vs pressure curves calculated for (a) (8,8), (b) (18,0) and (c) (24,0) bundled SWNTs. The pressure evolution for (10,0) SWNT is similar to (8,8) SWNT showed in (a) and the circular-oval and oval-peanut transitions is found close to 1.55 and 9.6 GPa

As expected, the critical pressures are strongly diameter-dependent^{11,18,20,27,36,37}. Actually, many authors have pointed out that the critical pressure (p_1) for circular-oval transition scales with d_t^{-3} , where d_t is tube diameter.¹¹ Some authors also found that the critical pressure for oval-peanut transition (p_2) also scales with d_t^{-3} .^{27,38} Our results for bundled SWNTs shown in Fig 1 point out that the transition to the peanut geometry (p_2 and p'_2) follows approximately the same law $p_2 = C/d_t^3$ with $C=4.4\text{nm}^3.\text{GPa}$. This scaling law was observed for all studied zigzag and armchair bundled tubes. However, the pressure transition values p_1 e p'_1 for circular to intermediate phase (oval and polygonal, respectively) show a slightly dependence on the inverted tube diameter but they do not follow the d_t^{-3} scaling law.

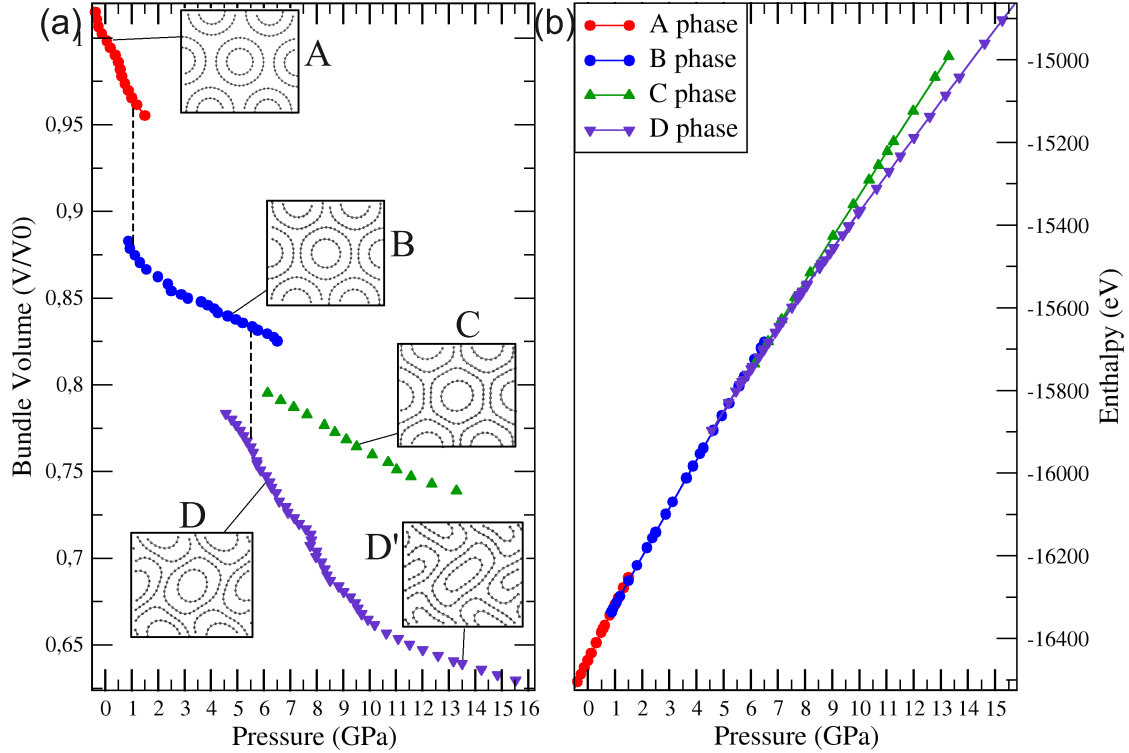


FIG. 2. p - V curves (a) and enthalpy functions (b) for the pressure-induced sequence of phase transitions in the $(10,0)@(18,0)$ DWNT. Different cross-sectional shapes correspond to different colors in the plots and are shown in the insets.

We also have modeled several DWNT bundles under pressure and choose the $(10,0)@(18,0)$ DWNT (This notation means that the $(10,0)$ tube is inside the $(18,0)$ tube) in order to compare its structural stability with those of their constituent SWNTs. We find a very similar behavior for the other DWNTs such $(12,0)@(20,0)$ and $(11,0)@(19,0)$. In Fig. 2a and 2b we show respectively the p - V and enthalpy curves for the $(10,0)@(18,0)$ DWNT bundle. Upon compressing the original circular structure of a DWNT we find four distinct structures as shown in Fig. 2a. The A configuration is the non-deformed structure with a circular shape for both inner and outer tube. The B configuration is characterized by the polygonization of the outer tube while the inner tube maintain its circular cross section. The C configuration corresponds to a polygonal outer tube and oval inner tube. Finally, the D configuration stands for the case where the outer and inner tubes display oval/peanut cross-sectional shapes.

The polygonization of outer tube (A - B phase transition) in $(10,0)@(18,0)$ DWNT bundle

is observed at 0.81 GPa which is lower than the value (1.2 GPa) what was calculated for the same transition in the (18,0) SWNT bundle. This result suggests that the presence of the inner tube enhances the outer-outer tube interactions within the bundle, thus reducing the critical pressure value for polygonization. Upon increasing the pressure, a B - C transformation occurs at 6.2 ± 0.2 GPa, since the inner tube ovalizes and the outer tube reaches a higher degree of polygonization. We are able to increase the pressure in the C phase up to 13 GPa without inducing any strong deformation. However, from the enthalpy analysis we conclude that the D phase is more stable than C phase for the whole range of investigated pressures. Thus the C configuration is actually metastable. By further increasing the pressure in the D phase, it reaches the same enthalpy as the B phase around 5.7 ± 0.2 GPa. The D phase is also metastable even at lower pressures, down to 5.5 GPa. In summary, the actual sequence of phase transitions for the (10,0)@(18,0) DWNT bundle is $A \rightarrow B$ at 0.81 GPa and $B \rightarrow D$ at 5.7 ± 0.2 GPa. This value contrasts with the 1.4 GPa calculated collapse pressure of the (18,0) SWNT outer tube, clearly pointing out to the structural support given by the inner tube, as already proposed by some authors^{29,30}.

We conclude that the C configuration (polygonized outer tube and ovalized inner tube) is unstable when we compare with the both collapsed tubes which let us propose that the ovalization of the inner tube is the reason for the overall collapsing of DWNT. For isolated DWNTs, Ye et al²⁸ suggest that the DWNT transition could be essentially determined by the inner tube transition. They also found that collapse of DWNTs follow almost the same d_t^{-3} law when the inner tube is used, which means that p_c for DWNTs is the same as expected for SWNT inner tube²⁸. In such way, our results agrees in the fact that the inner tube ovalization determines the critical pressure for collapsing of DWNTs. However, there is a clear pressure screening effect from the outer tube in the behavior of the inner tube because the critical pressure for the expected circular-oval transition for inner tube was increased to 5.7 ± 0.2 GPa when it was encapsulated in the DWNT. This value is considerably higher than that observed for the (10,0) SWNT bundle, which was 1.55 GPa. Second, the full collapsing of the inner tube (oval-peanut transition) is continuous in the DWNT case, differently from the SWNT case, in which there is a discontinuous change in the volume (around 9.6 GPa). For the DWNT case, this transition is marked by a change in compressibility (which is proportional to the slope of the $p - V$ plot) at around 10 GPa, clearly seen from Fig.2. We found a similar behavior for (12,0)@(20,0) DWNT bundle, where

the transition $B \rightarrow D$ is predicted to occur at 5.5 ± 0.1 GPa and change in bulk modulus takes places around 5.9 GPa close to that value expected for (12,0) SWNT (5.4 GPa).

B. Phonon Density of States evolution under pressure

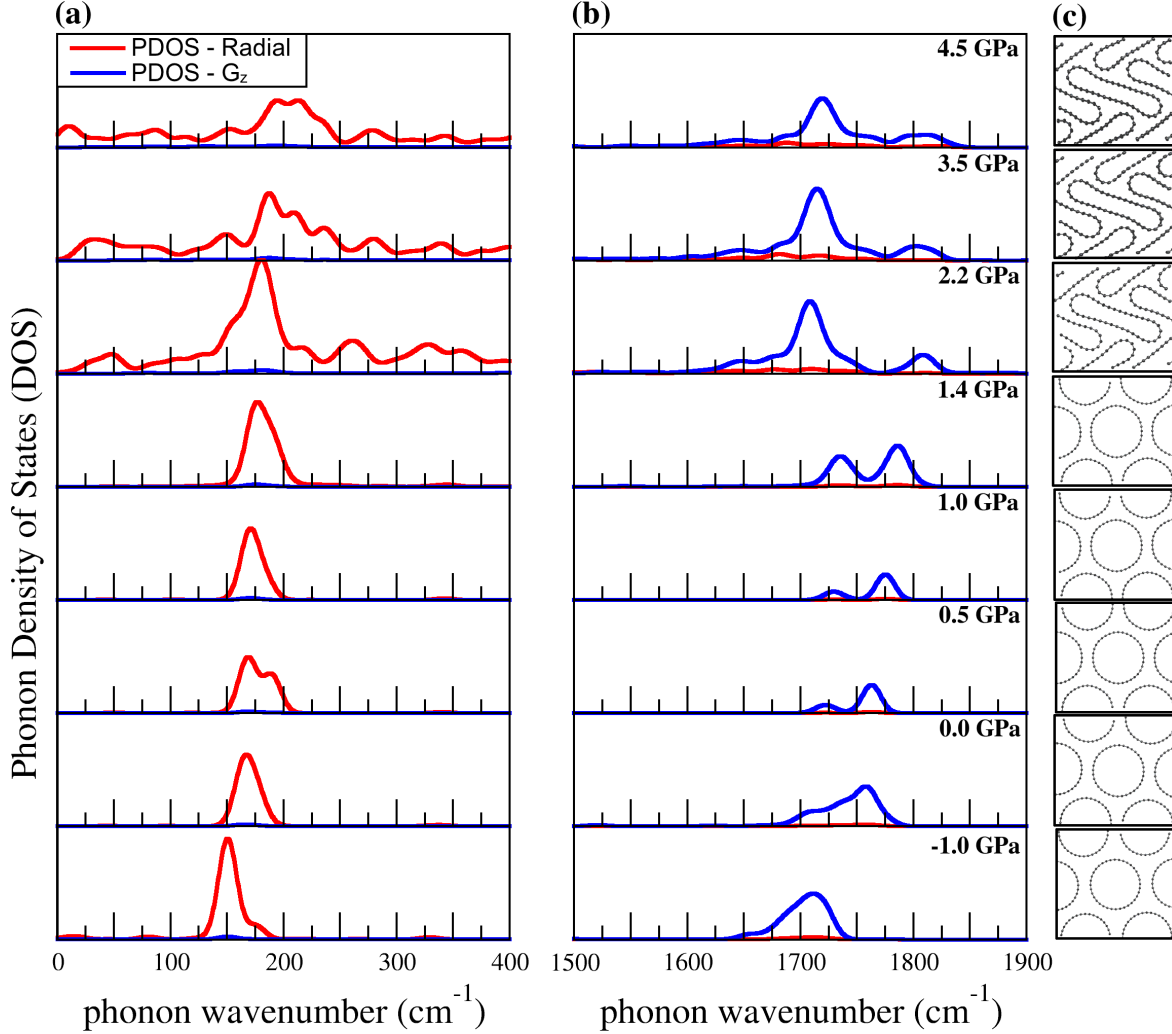


FIG. 3. Phonon density of states (DOS) projected in RBM (a) and tangential (b) probing vectors for (18,0) SWNT. Some snapshots of the bundle structure evolution can be followed in (c).

Fig 3 shows the phonon projected density of states (PDOS) calculated for (18,0) SWNT bundles. The PDOS for RBM and G_z modes are shown in red (a) and blue (b), respectively. From the figure, we can follow the RBM and G_z evolutions as pressure is increased, and the corresponding snapshots of the bundle structural evolution are shown in the right panels. First, we observe the RBM mode of (18,0) SWNT in the low frequency region centered at

around 150 cm^{-1} in the circular phase (0.0 GPa), which gradually shifts to higher frequencies as the pressure is increased. The pressure coefficient of this mode is $7.0 \pm 2.5 \text{ cm}^{-1}/\text{GPa}$, in good agreement with experiments^{2,24,39}. After collapse, the contributions to the radial mode spread in the low frequency region, which is equivalent to say that the RBM is not a single, well-defined mode any longer in good correspondance with the experimental difficulty to observe RBM after the some suggested pressure phase transitions.^{2,3,27,40–42}

The G_z band behavior is shown in the right panel. We clearly observe the splitting of this mode when polygonization takes place. After collapse, we clearly see a sudden jump to lower frequencies and intensity enhancement of the lower-frequency contribution, while the higher-frequency one continues to upshift. We studied several SWNTs bundles and similar results were observed. For (10,0) SWNT bundle the spread of radial contribution were observed in circular-oval transition i.e. before the collapsing of tube. The split of G_z component due polygonization is also observed for (24,0) SWNT bundle and, evidently, not observed for (10,0) SWNT. Furthermore, the sudden red-shift of G_z component after collapsing is also observed for (24,0) SWNT.

The phonon evolution with pressure for (10,0)@(18,0) DWNT bundle can be observed in Fig 4. It is clear from left panels the presence in low-frequency region of two distinct peaks around 150 cm^{-1} and 325 cm^{-1} corresponding to RBM modes of outer and inner tubes, respectively. The peaks are slightly shifted from the corresponding SWNTs in the circular conformation, as expected from the intertube coupling⁴³. It is interesting to note the evolution of both RBM peaks with pressure, where we clearly observe that the RBM frequency of the outer tube shifts much faster than the RBM frequency of the inner tube before collapse. This is a clear evidence of a screening effect on the inner tube by outer tube. Pressure screening effects on RBM and G band in DWNTs have been observed in several Raman experiments^{13,17,44–46}. Our calculations of RBM and G_z confirm that this pressure screening effect occurs well before any structural collapse. In the (b) panels of Fig. 4, we can follow the G_z component for outer and inner tube. It should be noted here that inner (10,0) tube G_z component is well overestimated being at about 1850 cm^{-1} compared with the outer (18,0) one which is located at around 1650 cm^{-1} . However, qualitative analysis could be still performed. It is interesting to note that pressure screening effects are also observed in tangential components as we can see that the outer tube G_z components shift faster than the inner ones. As observed for SWNTs, the transition of the outer tube to a

polygonized phase at 0.85 GPa is clearly marked by a splitting of the G_z band. After collapse, the PDOS spreads over a large frequency range for radial and tangential contributions but it is possible to see that the lowest frequency components of G_z are suddenly shifted to lower frequencies, as in the case of SWNTs bundles.

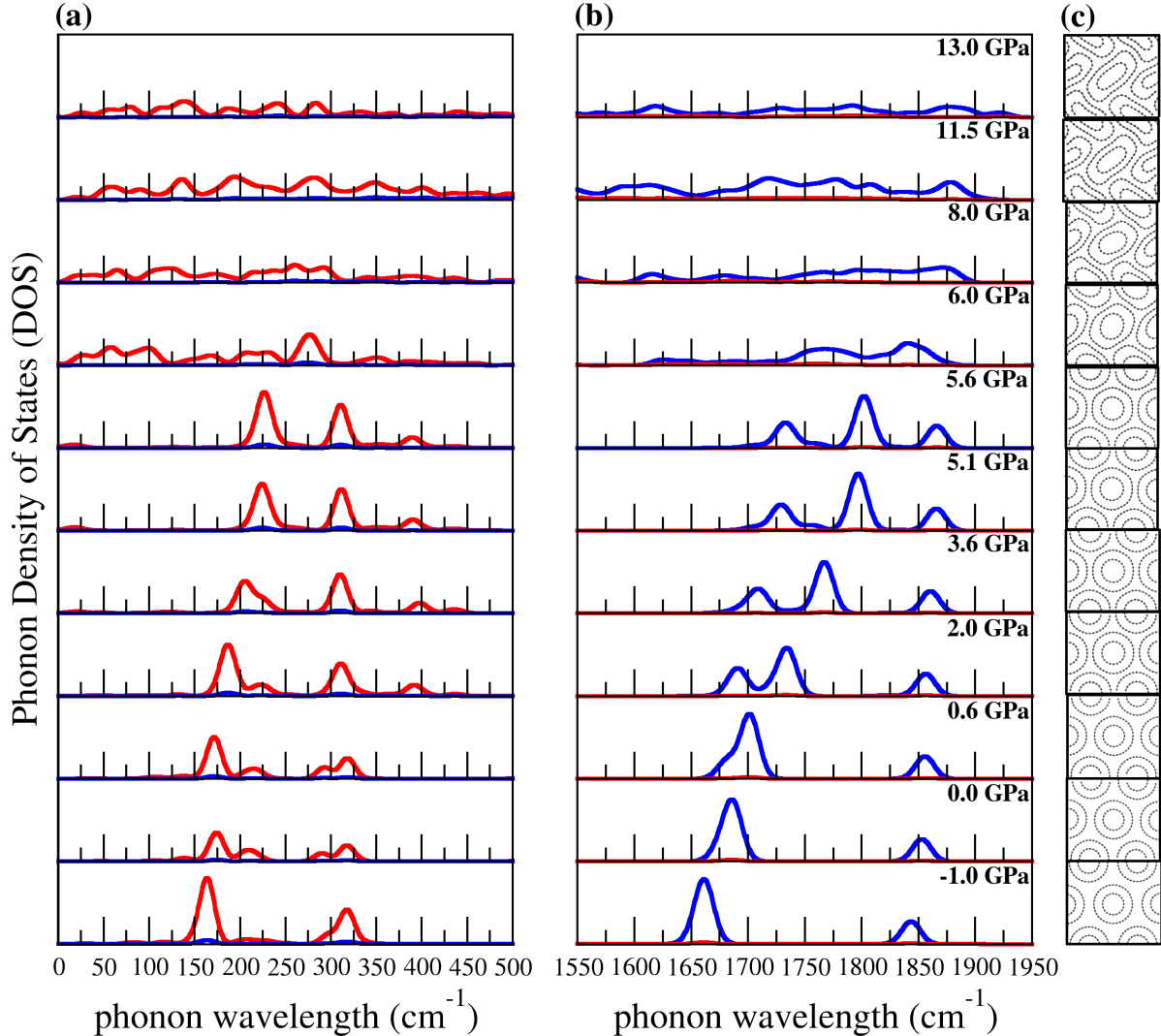


FIG. 4. Phonon density of states (DOS) projected in RBM (a) and tangential (b) probing vectors for (10,0)@(18,0) DWNT. Some snapshots of bundle evolution can be followed in (c).

In Fig. 5, we plot the z-displacement i.e., along the tube axis direction, of some eigenvectors as a function of the coordinate angle θ defined from the center of (18,0) tube. First, we have identified the A_{1g} mode centered around 1721.4 cm⁻¹ for the structure at -1.0 GPa (Fig. 5a). This is the mode which mainly contributes to v-PDOS as we can see in Fig. 5b. As the pressure is increased up to 1.4 GPa, the (18,0) cross section is polygonized as we

observe a split of G_z PDOS contribution. Analysis of the phonon displacements (Fig. 5a) shows that the higher frequency component is mainly due to modes which are localized on the high-curvature regions (vertices of the hexagons). Modes centered at 1771.3, 1780.7 and 1786.1 cm^{-1} have the same symmetry and their maximums of displacement are localized for θ equal to $\pm 30^\circ$, $\pm 90^\circ$ and $\pm 150^\circ$ which are the vertices of polygonized shape. After the collapse of (18,0) SWNT bundle, we have calculated phonon eigenvectors for collapsed structure at 2.2 GPa. In Fig. 5a, we show modes centered at 1800.6, 1803.2 and 1815.4 cm^{-1} which mainly contribute to higher-frequency peak in PDOS. Then, we clearly see that high-frequency contribution in PDOS at 2.2 GPa come from modes that are localized in the high-curved regions of the peanut-shaped tube. ($\theta \sim \pm 180^\circ$ and $\theta \sim \pm 0^\circ$). Consequently, the low-frequency and more intense peak of PDOS is due to vibration modes which are localized in the flat regions of the peanut-shaped structure.

From an experimental point of view, it has been recently proposed that a saturation or even a negative pressure slope of Raman G^+ component for SWNT and DWNT could be associated to the collapse of the nanotubes^{5,17,39}. Furthermore, after the collapse this band follows the graphite pressure evolution as observed in Fig. 6. with a smaller pressure coefficient^{17,47}. This was also observed in PDOS of SWNT bundle calculations (cf. Fig 3b). Our calculations confirm this hypothesis and identifies the atomistic origin of the low-frequency bands. Collapsing of the nanotube cross-section leads to flattened regions where the reduced stress in C-C tangential bonds reduce the G_z frequency. However, as we observe in our calculations, a small high-frequency component of G_z component, arising from the high-curvature regions, remains after the collapse. Since the flattened portion of the tubes is much higher than curved portion, we expect that the low-frequency shift of the G band is dominant in the experiments. The experimentally red-shift observed of the G-band is then explained from our calculations as related to the dominance of the flat region of the collapse phase in the Raman signal. This is in addition perfectly coherent with the fact in the collapsed state the pressure evolution of the G-band clearly matches (see Fig. 6) the one of graphite or graphene under triaxial compression^{47,48}.

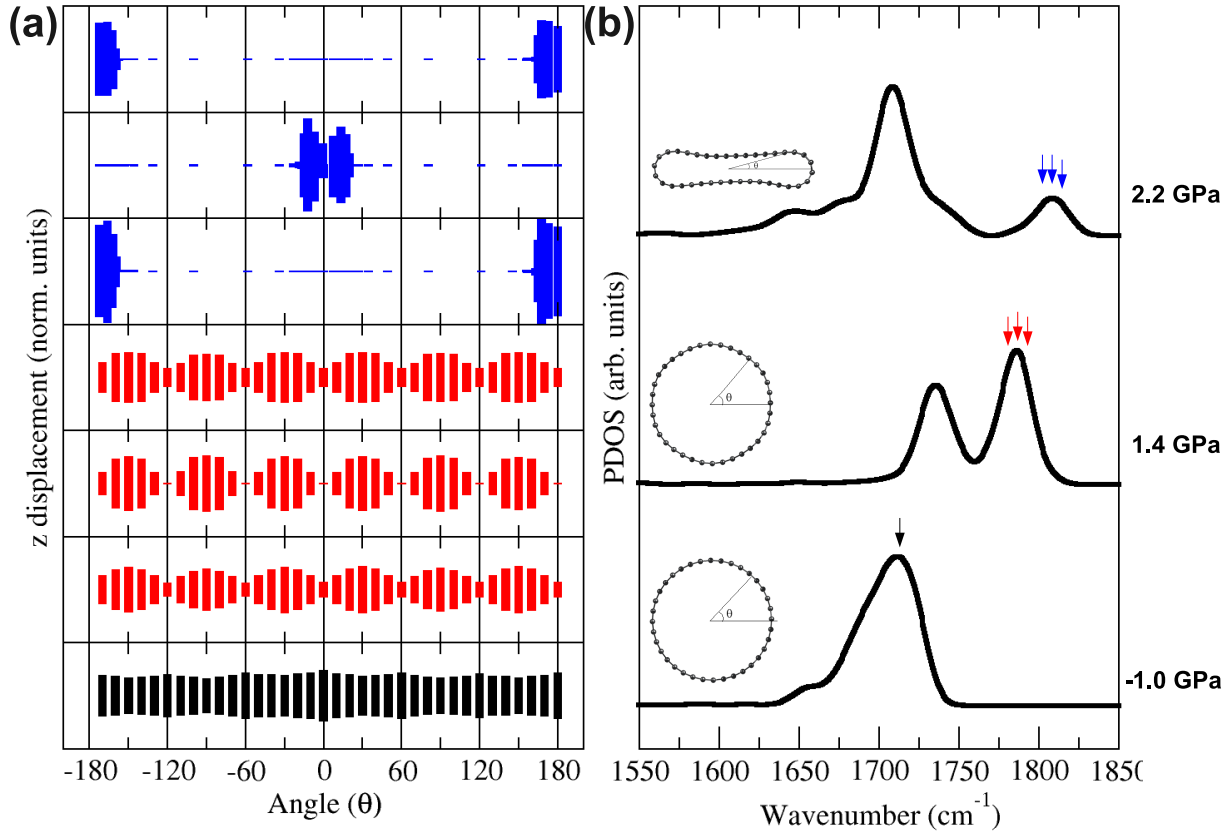


FIG. 5. (a) Amplitude of z-displacements of (18,0) SWNT bundle as a function of coordinate angle before the collapse (-1.0 GPa and 1.4 GPa) and after collapse (2.2 GPa). From bottom to top: Eigenvectors for A_{1g} mode centered at 1721.4 cm^{-1} (black) at -1.0 GPa; for modes centered at 1771.3 , 1780.7 and 1786.1 cm^{-1} (red) at 1.4 GPa, and for modes centered at 1800.6 , 1803.2 and 1815.4 cm^{-1} (blue) at 2.2 GPa. (b) v-PDOS projected in z direction for (18,0) SWNT at -1.0, 1.4 and 2.2 GPa. Arrows mark the center of modes whose eigenvectors are plotted in (a).

IV. CONCLUSIONS

We studied high-pressure structural modifications and phonon-mode shifts of single and double wall carbon nanotubes bundles using zero-temperature enthalpy minimization with classical interatomic potentials. We confirmed that the structural transformation of SWNTs in bundles from circular to collapsed cross-section under hydrostatic pressure is strongly diameter-dependent. It is also evident that the transition from polygonized to collapsed cross section for large diameter tubes has a first-order character with a large bundle volume discontinuity whereas for small diameters the transition is continuous, with intermediate oval

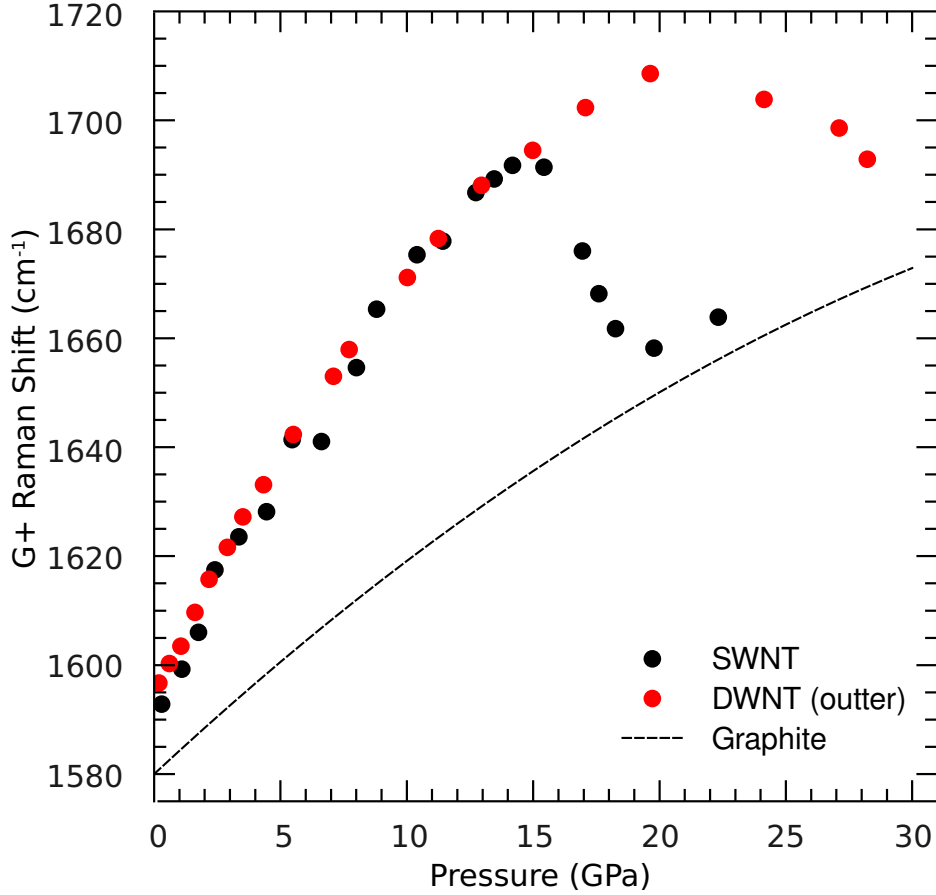


FIG. 6. Experimentally pressure Raman shift evolution of G^+ component for SWNTs, DWNT and graphite. Adapted from Ref.^{17,39,47,48}

or racetrack cross sections. For DWNT bundles, screening pressure effects were observed on the inner tube, which keeps its circular cross section for higher pressures than would be expected from the SWNTs behavior. Furthermore, the inner tube acts as structural support to outer tube. Phonons calculation also reveals screening effects in radial and tangential component as the pressure increases. Polygonization of (18,0) SWNT bundle is characterized by a split of G_z PDOS contribution which is mainly due to localized modes on high-curved region of polygonal shape. After the collapse transition, the tangential modes associated with the flat regions of the tubes are suddenly shifted to low frequencies and high-curved contribution of peanut shape is less pronounced but still observed in G_z PDOS. The experimentally observation of the G-band red-shift at nanotube collapse let us conclude on the dominance on the Raman signal of collapsed tubes of the flat regions of collapsed tubes.

Moreover, this provides a coherent explanation of the lower pressure slope ($\sim 4\text{cm}^{-1}/\text{GPa}$) of the G-band observed after nanotubes collapse. Consequently, the pressure slope could be a useful means for the identification of the geometry shape state of SWNT and DWNTs.

ACKNOWLEDGEMENTS

The authors acknowledge CAPES-COFECUB collaboration program (grant 608) grant for the partial support of this research.

-
- ¹ Jie Tang, Lu-Chang Qin, Taizo Sasaki, Masako Yudasaka, Akiyuki Matsushita, and Sumio Iijima. Compressibility and polygonization of single-walled carbon nanotubes under hydrostatic pressure. *Phys. Rev. Lett.*, 85:1887–1889, Aug 2000.
 - ² M. J. Peters, L. E. McNeil, J. Ping Lu, and D. Kahn. Structural phase transition in carbon nanotube bundles under pressure. *Phys. Rev. B*, 61:5939–5944, 2000.
 - ³ Sukanta Karmakar, Surinder M Sharma, P V Teredesai, D V S Muthu, A Govindaraj, S K Sikka, and A K Sood. Structural changes in single-walled carbon nanotubes under non-hydrostatic pressures: x-ray and raman studies. *New Journal of Physics*, 5(1):143, 2003.
 - ⁴ A. Merlen, N. Bendiab, P. Toulemonde, A. Aouizerat, A. San Miguel, J. L. Sauvajol, G. Montagnac, H. Cardon, and P. Petit. Resonant raman spectroscopy of single-wall carbon nanotubes under pressure. *Phys. Rev. B*, 72(3):035409, 2005.
 - ⁵ Mingguang Yao, Zhigang Wang, Bingbing Liu, Yonggang Zou, Shidan Yu, Wang Lin, Yuanyuan Hou, Shoufu Pan, Mingxing Jin, Bo Zou, Tian Cui, Guangtian Zou, and B. Sundqvist. Raman signature to identify the structural transition of single-wall carbon nanotubes under high pressure. *Phys. Rev. B*, 78(20):205411, Nov 2008.
 - ⁶ J. C. Charlier, Ph. Lambin, and T. W. Ebbesen. Electronic properties of carbon nanotubes with polygonized cross sections. *Phys. Rev. B*, 54(12):R8377–R8380, Sep 1996.
 - ⁷ T. Yildirim, O. Gulseren, C. Kilic, and S. Ciraci. Pressure-induced interlinking of carbon nanotubes. *Phys. Rev. B*, 62:12648–12651, Nov 2000.
 - ⁸ Marcel H. F. Sluiter, Vijay Kumar, and Yoshiyuki Kawazoe. Symmetry-driven phase transformations in single-wall carbon-nanotube bundles under hydrostatic pressure. *Phys. Rev. B*,

- 65:161402, Apr 2002.
- ⁹ S. Reich, C. Thomsen, and P. Ordejón. Elastic properties of carbon nanotubes under hydrostatic pressure. *Phys. Rev. B*, 65:153407, 2002.
- ¹⁰ R. B. Capaz, C. D. Spataru, P. Tangney, M. L. Cohen, and S. G. Louie. Hydrostatic pressure effects on the structural and electronic properties of carbon nanotubes. *phys. stat. sol.(b)*, 241:3352–3359, 2004.
- ¹¹ P. Tangney, R. B. Capaz, C. D. Spataru, M. L. Cohen, and S. G. Louie. *Nano Letters*, 5(11), 2005.
- ¹² I H Choi, P Y Yu, P Tagney, and S G Louie. Vibrational properties of single walled carbon nanotubes under pressure from raman scattering experiments and molecular dynamics simulations. *Physica Status Solidi*, 244(1):121–126, 2007.
- ¹³ J. Arvanitidis, D. Christofilos, K. Papagelis, K. S. Andrikopoulos, T. Takenobu, Y. Iwasa, H. Kataura, S. Ves, and G. A. Kourouklis. Pressure screening in the interior of primary shells in double-wall carbon nanotubes. *Phys. Rev. B*, 71(12):125404, 2005.
- ¹⁴ P Puech, E Flahaut, A Sapelkin, H Hubel, DJ Dunstan, G Landa, and WS Bacsa. Nanoscale pressure effects in individual double-wall carbon nanotubes. *Phys. Rev. B*, 73(23), 2006.
- ¹⁵ P Puech, A Chandour, A Sapelkin, C Tinguely, E Flahaut, D J Dunstan, and W Basca. Raman g band in double-wall carbon nanotubes combining p doping and high pressure. *Phys. Rev. B*, 78:045413, 2008.
- ¹⁶ S. Kawasaki, Y. Kanamori, Y. Iwai, F. Okino, H. Touhara, H. Muramatsu, T. Hayashi, Y. A. Kim, and M. Endo. Structural properties of pristine and fluorinated double-walled carbon nanotubes under high pressure. *J. Phys. Chem. Solids*, 69(5-6):1203–1205, MAY-JUN 2008. 14th International Symposium on Intercalation Compounds (ISIC 14), Seoul, SOUTH KOREA, JUN 12-15, 2007.
- ¹⁷ A. L. Aguiar, E. B. Barros, R. B. Capaz, A. G. Souza Filho, P. T. C. Freire, J. Mendes Filho, D. Machon, Ch. Caillier, Y. A. Kim, H. Muramatsu, M. Endo, and A. San-Miguel. Pressure-induced collapse in double-walled carbon nanotubes: Chemical and mechanical screening effects. *Journal of Physical Chemistry C*, 115:5378–5384, 2011.
- ¹⁸ Ali Nasir Imtani and V. K. Jindal. Structure of armchair single-wall carbon nanotubes under hydrostatic pressure. *Phys. Rev. B*, 76(19):195447, Nov 2007.

- ¹⁹ Ali Nasir Imtani and V. K. Jindal. Bond lengths of armchair single-walled carbon nanotubes and their pressure dependence. *Computational Materials Science*, 44:156–162, 2008.
- ²⁰ Ali Nasir Imtani and V. K. Jindal. Structure of chiral single-walled carbon nanotubes under hydrostatic pressure. *Computational Materials Science*, 46:297–302, 2009.
- ²¹ W. Yang, R Z Wang, X M Song, B Wang, and H Yan. Pressure-induced raman-active radial breathing mode transition in single-wall carbon nanotubes. *Phys. Rev. B*, 75:045425, 2007.
- ²² Marcel H. F. Sluiter and Yoshiyuki Kawazoe. Phase diagram of single-wall carbon nanotube crystals under hydrostatic pressure. *Phys. Rev. B*, 69(22):224111, Jun 2004.
- ²³ D Christofilos, J Arvanitidis, C Tzampazis, K Papagelis, T Takenobu, Y Iwasa, H Kataura, C Lioutas, S Ves, and G A Kourouklis. Raman study of metallic carbon nanotubes at elevated pressure. *Diamond and Related Materials*, 15:1075–1079, 2006.
- ²⁴ A. Merlen, P. Toulemonde, N. Bendiab, , A. Aouizerat, J. L. Sauvajol, G. Montagnac, H. Cardon, P. Petit, and A. San Miguel. Raman spectroscopy of open-ended single wall carbon nanotubes under pressure: effect of the pressure transmitting medium. *Phys. Stat. Sol.*, 243(3):690–699, 2006.
- ²⁵ J E Proctor, M P Halsall, A Ghandour, and D J Dunstan. Raman spectroscopy of single-walled carbon nanotubes at high-pressures: Effect of interaction between the nanotubes and pressure transmitting media. *Phys. Stat. Sol.*, 244(1):147–150, 2007.
- ²⁶ A. Abouelsayed, K Thirunavukkuarasu, F Hennrich, and C A Kuntscher. Role of the pressure transmitting medium for the pressure effects in single-walled carbon nanotubes. *Journal of Physical Chemistry C*, 114:4424–4428, 2010.
- ²⁷ James A. Elliott, Jan K. Sandler, Alan H. Windle, Robert J. Young, and Milo S. Shaffer. *Phys. Rev. Lett.*, 92, 2004.
- ²⁸ X. Ye, D. Y. Sun, and X. G. Gong. Pressure-induced structural transition of double-walled carbon nanotubes. *Phys. Rev. B*, 72:035454, Jul 2005.
- ²⁹ X Yang, G Wu, and J Dong. Structural transformations of double-wall carbon nanotubes bundle under hydrostatic pressure. *Applied Physics Letters*, 89(113101):113101–113103, 2006.
- ³⁰ Vikram Gadagkar, Prabal K. Maiti, Yves Lansac, A. Jagota, and A. K. Sood. Collapse of double-walled carbon nanotube bundles under hydrostatic pressure. *Phys. Rev. B*, 73(8):085402, Feb 2006.

- ³¹ Donald W Brenner, Olga A Shenderova, Judith A Harrison, Steven J Stuart, Boris Ni, and Susan B Sinnott. A second-generation reactive empirical bond order (rebo) potential energy expression for hydrocarbons. *Journal of Physics: Condensed Matter*, 14(4):783, 2002.
- ³² D. W. Brenner. Empirical potential for hydrocarbons for use in simulating the chemical vapor deposition in diamond films. *Phys. Rev. B*, 42(15), 1990.
- ³³ J. C. Charlier, Ph. Lambin, and T. W. Ebbesen. Electronic properties of carbon nanotubes with polygonized cross sections. *Phys. Rev. B*, 54(12):R8377–R8380, Sep 1996.
- ³⁴ J.Z. Liu, Q.-S. Zheng, L.-F. Wang, and Q. Jiang. Mechanical properties of single-walled carbon nanotube bundles as bulk materials. *Journal of the Mechanics and Physics of Solids*, 53(1):123 – 142, 2005.
- ³⁵ C. Q. Ru. Effective bending stiffness of carbon nanotubes. *Phys. Rev. B*, 62(15):9973–9976, Oct 2000.
- ³⁶ Lorin X. Benedict, Nasreen G. Chopra, Marvin L. Cohen, A. Zettl, Steven G. Louie, and Vincent H. Crespi. Microscopic determination of the interlayer binding energy in graphite. *Chemical Physics Letters*, 286:490–496, 1998.
- ³⁷ D. Y. Sun, D. J. Shu, M. Ji Feng Liu, M. Wang, and X. G. Gong. *Phys. Rev. B*, 70, 2004.
- ³⁸ Jian Wu, Ji Zang, Brian Larade, Hong Guo, X. G. Gong, and Feng Liu. Computational design of carbon nanotube electromechanical pressure sensors. *Phys. Rev. B*, 69:153406, Apr 2004.
- ³⁹ Ch. Caillier, D. Machon, A. San-Miguel, R. Arenal, G. Montagnac, H. Cardon, M. Kalbac, M. Zukalova, and L. Kavan. Probing high-pressure properties of single-wall carbon nanotubes through fullerene encapsulation. *Physical Review B*, 77(12):125418, 2008.
- ⁴⁰ J. Sandler, M. S. P. Shaffer, A. H. Windle, M. P. Halsall, M. A. Montes-Morán, C. A. Cooper, and R. J. Young. Variations in the raman peak shift as a function of hydrostatic pressure for various carbon nanostructures: A simple geometric effect. *Phys. Rev. B*, 67:035417, Jan 2003.
- ⁴¹ P. T. C. Freire, V. Lemos, J. A. Lima, G. D. Saraiva, P. S. Pizani, R. O. Nascimento, N. M. P. S. Ricardo, J. Mendes Filho, and A. G. Souza Filho. Pressure effects on surfactant solubilized single-wall carbon nanotubes. *physica status solidi (b)*, 244(1):105–109, 2007.
- ⁴² John E. Proctor, Matthew P. Halsall, Ahmad Ghandour, and David J. Dunstan. High pressure raman spectroscopy of single-walled carbon nanotubes: Effect of chemical environment on individual nanotubes and the nanotube bundle. *Journal of Physics and Chemistry of Solids*, 67(12):2468–2472, 2006.

- ⁴³ V. N. Popov and Luc Henrard. Breathinglike phonon modes of multiwalled carbon nanotubes. *Phys. Rev. B*, 65:235415, May 2002.
- ⁴⁴ D Christofilos, J. Arvanitidis, G. A. Kourouklis, S. Ves, T. Takenobu, Y Iwasa, and H. Kataura. Identification of inner and outer shells of double-wall carbon nanotubes using high pressure raman spectroscopy. *Phys. Rev. B*, 76, 2007.
- ⁴⁵ P. Puech, H. Hubel, D. J. Dunstan, R. R. Bacsa, C. Laurent, and W. S. Bacsa. Discontinuous tangential stress in double wall carbon nanotubes. *Phys. Rev. Lett.*, 93(9):095506, 2004.
- ⁴⁶ P Puech, H Hubel, D J Dunstan, A Bassil, R Bacsa, A Peigney, E Flahaut, C Laurent, and W S Basca. Light scattering of double wall carbon nanotubes under hydrostatic pressure: pressure effects on the internal and external tubes. *phys. stat. sol.(b)*, 241:3360–3366, 2004.
- ⁴⁷ M. Hanfland, H. Beister, and K. Syassen. Graphite under pressure: Equation of state and first-order raman modes. *Phys. Rev. B*, 39:12598–12603, Jun 1989.
- ⁴⁸ Jimmy Nicolle, Denis Machon, Philippe Poncharal, Olivier Pierre-Louis, and Alfonso San-Miguel. Pressure-mediated doping in graphene. *Nano Letters*, 11(9):3564–3568, 2011.